Density-functional investigation of gold-coated metallic nanowires

S. Gemming,[1,2] G. Seifert,[1] and M. Schreiber[2]

[1]*Institut für Physikalische Chemie und Elektrochemie, Technische Universität Dresden, Mommsenstrasse 13, D-01062 Dresden, Germany*

[2]*Institut für Physik, Technische Universität Chemnitz, D-09107 Chemnitz, Germany*

Density-functional band-structure calculations were carried out for two-shell metallic nanowires from Au and from AgAu and PdAu alloys. All structures are local minima of the formation energy, and more stable than the unreconstructed, planar Au(111) surface. The most stable structure contains nine atoms in the repeat unit along the wire direction, and its stability increases in the order $PdAu_8 < Au_9 < AgAu_8$. This trend coincides with the tensile stress acting on the central monatomic chain. An analysis of the electronic structure shows that the binding between the two shells is not strongly directional, especially in the alloyed wires. The interatomic interaction along the central chain is weakened, thus the tensile stress along this direction is alleviated. In Au_9 and $AgAu_8$ eight s bands constitute the conductance channels for ballistic electron transport. For the Pd-centered wire only the conductance channels from the Au_8 shell are present, whereas the central one is depopulated. These findings rationalize the lower conductivity of PdAu contacts compared with AgAu contacts obtained recently by break-junction experiments.

PACS number(s): 73.22.−f, 73.20.At, 73.63.Rt

I. INTRODUCTION

The PdAu alloy is widely used as a contact metal in microelectronic devices. Hence, the physical properties of the bulk alloy,[1–5] some surfaces,[6–8] and mixed, alloyed clusters[9] have been experimentally and theoretically analyzed in great detail as a function of the alloy composition. Also mixed silver-gold nanoparticles have acquired widespread interest in microelectronics[10] and biotechnology.[11] For the AgAu system even elongated core-shell particles $Ag_{core}Au_{shell}$ and $Ag_{core}Ag_{shell}$, can be prepared,[12–14] and converted into alloyed nanoparticles by irradiation with laser pulses.[10] Cluster-size effects on electronic and optical properties of alloyed structures are more prominent than the dependence on the chemical composition.[14–16] However, density-functional band-structure calculations for thin, long bimetallic nanowires suggest, that a miscibility gap occurs in the AgAu phase diagram for wires with higher Ag content,[17] whereas wires with low Ag content exhibit a stabilization compared with the pure Ag or Au wires.

For nanojunctions of AgAu and PdAu alloys quantized conductance was measured.[18,19] In AgAu alloys, the $1G_0$ peak in the conductance histogram is observed throughout the full composition range, whereas the peak significantly loses intensity for the higher Pd concentrations of the PdAu alloy. It was concluded that Au atoms are repelled from the nanoconstriction, such that a monatomic or diatomic nanocontact of Ag or Pd forms the break junction. It was proposed that the low s/p valency of a Pd atom hinders the s/p-type conductivity through an atomic Pd junction, whereas the analogous Ag junction should exhibit similar properties as a monatomic Au junction. It is the scope of the present study to investigate this hypothesis by electronic structure calculations of thin nanowires within a density-functional band-structure framework.

II. COMPUTATIONAL DETAILS

The structural and electronic properties of the gold and gold-coated nanowires were investigated by local density-functional band-structure calculations[20–23] with the program ABINIT.[24] Self-consistent total energies and forces were employed to optimize the atom arrangement of the nanowires within three-dimensionally periodic boundary conditions. Flat supercells of 12.7 Å × 12.7 Å × c were employed, where c roughly equals one or two bond distances (see Sec. III). This supercell size ensures that the interaction between an (8,0) wire and its neighboring periodic replica is lower than a threshold of 1 meV/atom, and even less for the thinner (8,4) and (6,3) wires. Band structures, densities of electronic states, and valence-electron densities were used to analyze the electronic properties of the most stable nanowire structures.

The core-valence interactions were described by norm-conserving pseudopotentials for the configurations $[Kr]5s^{0.5}4d^{9.5}$ of Pd, $[Kr]5s^14d^{10}$ of Ag, and $[Xe]6s^15d^{10}$ for Au.[25] In accordance with previous studies[26] a plane-wave cutoff of 810 eV was employed. For an accuracy of the total energy of better than 1 meV a k-point sampling of 16 to 32 intersections along the Γ-Z direction was employed in the structure optimization. For a more pictorial representation of the electronic structure electron density difference maps are displayed.

III. NANOWIRE STABILITY

A. Geometry

According to transmission electron microscopy measurements crystalline, nonchiral Au and Ag wires exhibit a high stability.[27,28] Indeed, in the absence of tensile stress three prototype two-shell nanowires of the noble metals and noble metal alloys are stable compared with the corresponding sur-
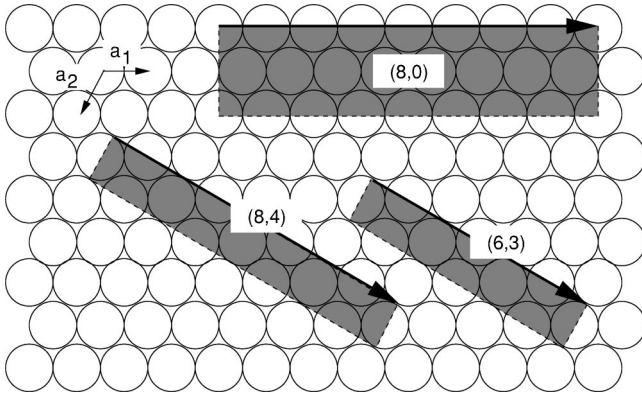
FIG. 1. Construction and nomenclature of the outer shell of the nanowires from a planar (111) monolayer. The areas shaded in grey denote the repeat unit of the cylindrical shell, the arrows indicate the vectors (m,n), which yield the coincident points.
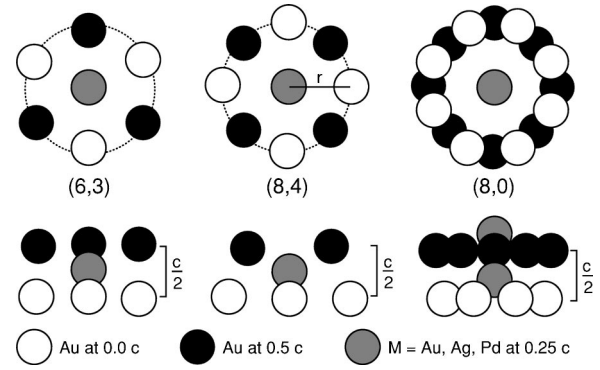

FIG. 2. Schematic representation of the atom arrangement within the supercell for the (6,3), (8,4), and (8,0) wires (from left to right). The upper part gives a top view, the lower one a side view of the wires. In (8,0) an additional M atom is located at $0.75\ c$.

face energies according to earlier density-functional calculations.[26,17] Thus, those wires attract particular attention, because they are the most promising candidates for an application as freestanding, not supported nanocontacts or elongated biochemical markers. Those wires consist of a central, straight, chain of equidistant atoms and a cylindrical outer shell, which is obtained by wrapping a metallic (111) monolayer around the central chain. The chiral structures and the orthorhombic distortion described in Ref. 26 are mainly stabilized by tensile stresses along the wire direction. The structures investigated in the present study are denoted as (6,3), (8,4), and (8,0). This nomenclature refers to the structure of the outer nanowire shell and gives the number of hexagonal lattice vectors, which yield coincident lattice points of the (111) monolayer, as depicted in Fig. 1.

In Fig. 2 the unit cells are displayed, which are repeated periodically to form the three different nanowires along the c direction. The thinnest (6,3) wire exhibits a threefold rotational symmetry, the medium-sized (8,4) wire a fourfold one, and the larger (8,0) even an eightfold one. These structural units are contained in supercells of length c along the wire direction and of width of 12.7 Å in the two directions perpendicular to the wire. For all three wire geometries this cell shape includes a sufficient amount of vacuum, such that the repetition by three-dimensionally periodic boundary conditions yields an interaction energy between a wire and its periodic replica of less than 1 meV/atom.

The experimentally observed conductivity differences occur for high Au concentrations. Furthermore, earlier density-

functional investigations indicated that the most stable alloyed structures occur in the gold-rich regime.[17] Thus, the present comparison of AgAu and PdAu alloys focuses on the compositions $M\mathrm{Au_6}$ for (6,3), $M\mathrm{Au_8}$ for (8,4), and $M_2\mathrm{Au_{16}}$ for (8,0), where $M=\mathrm{Au,Ag,Pd}$, M occupies the central straight chain, which is surrounded by an outer gold shell. In this way, gold-coated, "gilded" wires are obtained.

Table I gives an overview over the geometric parameters, which determine the wire structure: the radius r, which corresponds to the distance between the inner and outer shells, the supercell length c, and the distance d between two gold atoms of the outer $\mathrm{Au_8}$ shell. Regardless of the central atom the radii of the wires increase in the order $(6,3)<(8,4)<(8,0)$. For the (8,4) wires the distances between the atoms of the two shells are closest to the interatomic distance in the bulk crystals or alloys. Moreover, the distance c between neighboring atoms along the central chain is almost equal to the distance d between neighboring atoms on the outer shell, which leads to very symmetrical structures. The larger radii of the (8,0) wires are compensated by the shorter lengths c, and concomitantly to slightly shorter interatomic distances in the outer shell. For the thinner (6,3) wires the smaller radii are compensated by a relaxation of the outer shell along the wire direction, which leads to two different bond distances d of the outer shell. If the two layers brace an atom of the central chain (drawn in grey in Fig. 2) the corresponding distance is increased by an increment Δd, otherwise it is diminished by Δd. With values of 0.169 Å ($\mathrm{Au_7}$), 0.165 Å ($\mathrm{AgAu_6}$), and 0.165 Å ($\mathrm{PdAu_6}$) the

TABLE I. Radius r, length c, and interatomic distance d between the gold atoms of the outer shell (in Å) of the nine investigated nanowires, and the atom distance of the straight monatomic chains.

	r			c			d		
(n,m)	Au_{n+1}	AgAu_n	PdAu_n	Au_{n+1}	AgAu_n	PdAu_n	Au_{n+1}	AgAu_n	PdAu_n
(6,3)	2.587	2.557	2.549	2.671	2.680	2.700	2.670	2.646	2.630
							3.007	2.976	2.943
(8,4)	3.045	3.050	3.020	2.687	2.704	2.684	2.690	2.699	2.673
(8,0)	3.442	3.449	3.447	2.399	2.396	2.397	2.634	2.640	2.638
mono				2.492	2.568	2.367			

TABLE II. Formation energy [in eV/atom] with respect to the pure face-centered cubic bulk metals.

(n, m)	Au_{n+1}	$AgAu_n$	$PdAu_n$
(6,3)	0.53	0.47	0.61
(8,4)	0.44	0.40	0.51
(8,0)	0.54	0.52	0.61

increments are almost equal for all three central metals. In this way, two sets of distances d are obtained, such that the shorter one is roughly equal to the d values of the (8,0) wires and the longer one roughly equals the r value of the (8,4) wires.

Based on the lattice constants of the pure bulk face-centered cubic crystals (Pd: 3.89 Å, Ag: 4.06 Å, Au: 4.07 Å), equally long Ag-Au and Au-Au distances are expected, whereas the Pd-Au distances should be shorter by 4% for a given wire. However, in the very thin nanostructures studied here, such considerations derived from bulk data must be refined. First, the c and r values of the (8,4) wire do not exhibit any obvious correlation: the radius decreases from M=Ag over Au to Pd, whereas the length of Au_9 and $PdAu_8$ is virtually the same. This indicates that slightly different bonding mechanisms can play a role for this most bulklike structure, and that the Pd-Au bonding is more similar to the Au-Au interaction than to the Ag-Au one. For the (6,3) structure the decrease of r from Au over Ag to Pd is counterbalanced by an increase of c. Thus, the average number density per repeat unit volume is maintained. A similar crowding argument may be invoked for the correlation between the r and c values of the (8,0) wire, for which, however, the changes between the three metals are only marginal. This indicates that the nature of the central metal is of low importance for the structural properties of a wire, once the radius exceeds a certain threshold. With values of about 3.445 Å the radii of the (8,0) wires are presumably close to this threshold. In the last line of Table I, the optimum interatomic distance within a straight monatomic wire is displayed; the values are in very good agreement with the results of comparable calculations.[32] With a value of 2.37 Å the distance along the Pd chain is considerably shorter than the corresponding distances in the noble metals (Au: 2.49 Å, Ag: 2.57 Å). From a comparison with the values c of the two-shell wires, it can be concluded that the central metal chain is always under tensile stress in the gold-coated Pd wires. A crossover from compressive to tensile stress occurs between the (8,0) and (8,4) wires of Au and the AgAu alloy, and the lowest tensile stress acts on the gold-coated Ag chain.

B. Formation energy

The formation energy is obtained by subtracting the total energies of the bulk phases from the total energy of the nanowire in stoichiometric amounts. Table II gives a compilation of the formation energies of the nine different systems. All formation energies are positive, because the reference state, which is the bulk crystal, has a lower total energy per atom than a free-standing wire, which exposes a large surface area with strong deviations from the bulk coordination. However, these formation energies are within an energy range of 0.40 to 0.61 eV/atom, which is of the order of the surface energy (0.6 to 0.7 eV/atom) of the most stable unreconstructed (111) surface of gold.[26,29] Due to the large computational effort comparable data for the more stable herringbone reconstruction of the (111) surface is not available, yet. Recent tight-binding calculations on the herringbone structure provided geometric data in very good agreement with experimental results, but no absolute values for the surface energy.[30] Classical modeling of other dense-packed reconstructions, in particular the $(L \times \sqrt{3})$ Au(111) surfaces also yields surface energies comparable with the formation energies of the nanowires.[31] It is therefore concluded that all nine wires can coexist with the planar surface. The preferred structure is the (8,4) wire, the other two structures are less stable by 0.07 to 0.12 eV/atom.

As discussed earlier,[17] the gold-coated Ag chains are more stable than the corresponding pure Au wires for all investigated wire radii. The optimum length $c \approx 2.70$ Å of a free-standing Au_6 or Au_8 tube matches better with the optimum length $c=2.57$ Å of a monatomic Ag chain than with the length $c=2.49$ Å obtained for the monatomic Au chain. Thus, the two components of the Ag-centered wire match better and experience lower strain. Concomitant with this result, the stabilization of the Ag-centered wire over the Au-centered one decreases with decreasing length c and increasing radius r of the wire. For the gold-coated Pd chain the central chain experiences the lowest strain in the (8,0) wire. Nevertheless, the strained radial Pd-Au bonds destabilize this structure and the (8,4) wire is favored by 0.10 eV/atom. In comparison with the noble metal wires the heat of formation for all Pd-centered wires is higher by up to 0.14 eV/atom. These values indicate a reduced intershell binding strength in the PdAu structures.

To corroborate this analysis the binding energy E_b between the central chain and the outer shell is evaluated by subtracting the total energy of the unrelaxed fragments from the total energy of the most stable two-shell (8,4) wire. With values of $E_b(Au_9)=0.27$ eV/atom, $E_b(AgAu_8)=0.29$ eV/atom, and $E_b(PdAu_8)=0.31$ eV/atom a similarly strong binding is predicted in all three cases. If the relaxation of the free fragments is accounted for, the situation changes to $E_b(AgAu_8)=0.27$ eV/atom$>E_b(Au_9)=0.16$ eV/atom$>E_b(PdAu_8)=0.03$ eV/atom, where the main changes are due to the relaxation of the central chain. Thus, the analysis of the binding energy and the heat of formation consistently yield a lower binding strength in the PdAu wires than in the purely noble metal structures.

IV. ELECTRONIC PROPERTIES

A. Band structure

The electronic properties of the wires with an (8,4) atom arrangement in the outer shell will be discussed in more detail, because the systems Au_9, $AgAu_8$, and $PdAu_8$ exhibit the
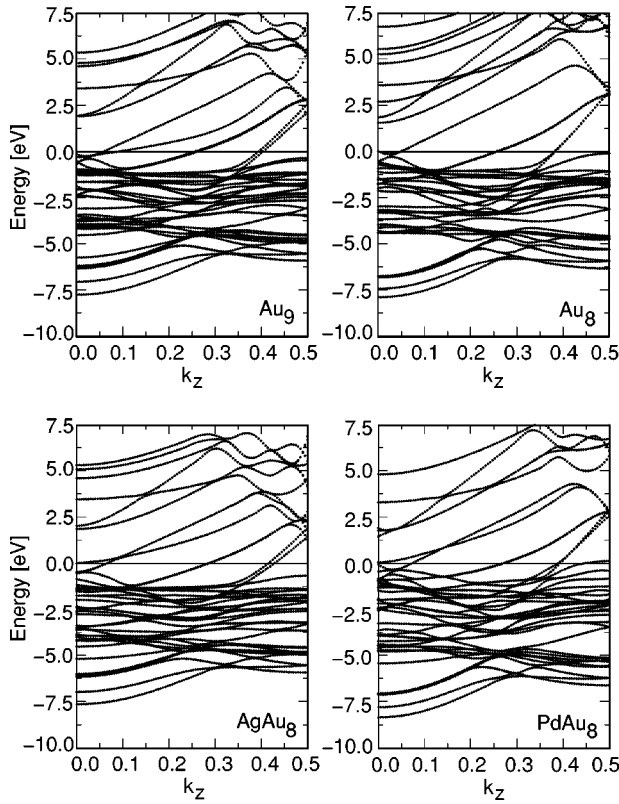
FIG. 3. Band structure along k_z for the pure wire Au_9, the Au_8 shell of that wire, the $PdAu_8$ wire, and the $AgAu_8$ wire clockwise from the upper left. The Fermi level is taken as zero point of the energy scale.

FIG. 4. Density difference maps for Au_9, $AgAu_8$, and $PdAu_8$ from top to bottom. The cut plane contains the central metal atom at $0.25 c$ and two further metal atoms at $0 c$. Three repeat units along the c direction are displayed. Depicted is the difference between the valence electron density of the two-shell wire and the sum of the valence electron densities of the outer shell and the inner monatomic wire. Areas of electron depletion are marked in black, electron accumulation is represented by the white. The contours span the range from -0.033 (black) to $+0.033$ (white) electrons/$Å^3$.

lowest formation energies, hence they are the most promising prototypes for an experimental realization. Figure 3 gives a representation of the electron bands along k_z of Au_9, the unfilled gold shell Au_8, $AgAu_8$, and $PdAu_8$. The occupied d levels exhibit a dispersion of about 8 eV at $k_z=0$ (Γ point) and of about 6.3 eV at $k_z=0.5$ (Z point). As shown previously[26] three doubly degenerate and two nondegenerate s-derived bands cross the Fermi level for Au_9. For the unfilled Au_8 shell the nondegenerate band with the lowest dispersion is missing, thus this most strongly localized band of Au_9 can be associated with the conductance channel of the central metal chain. Only minor changes occur for the remaining bands close to the Fermi level, the most prominent being the partial coincidence of the second nondegenerate band with an adjacent doubly degenerate one. This effect is caused by the higher symmetry of the unfilled Au_8 shell, which contains an axis of improper rotation, that is not present in the Au_9 wire. Additionally, close to the Z point a further band touches the Fermi level from below and substitutes the s-type conductance channel of the central chain with a d-type one.

For $AgAu_8$ the band of the central conductance channel intersects the Fermi level very close to the Γ point. The Ag d states are more strongly bound than the Au d states, but the expected downward shift of the levels is counterbalanced by reduced level splitting due to the larger atom distances. The repeat unit of the $PdAu_8$ wire contains one electron less than the units of the other two-shell wires. This has two effects on
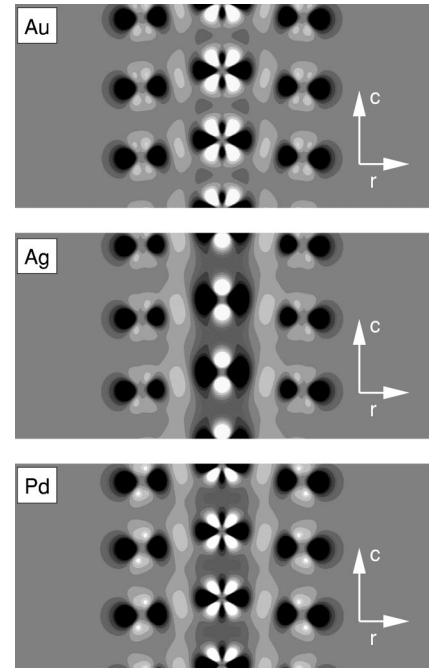
the band structure: First, the band of the central conductance channel touches the Fermi level at the Γ point and is unoccupied otherwise, and an occupied gold-derived d band becomes partially unoccupied close to the Z point Second, the band of the central Pd chain exhibits a significantly stronger dispersion than the corresponding, partially populated conductance channels of the Au_9 or the $AgAu_8$ wires, thus the electrons on the Pd chain are more strongly delocalized. The partial depopulation of the gold-derived d band is similar to the situation observed also for the Au_8 shell close to the Z point. Thus, the conductance channels of $PdAu_8$ resemble more the ones of the unfilled Au_8 shell with a weak contribution of the central channel close to the Γ point.

These findings rationalize the difference of the conductance measurements on PdAu and AgAu break junctions.[18,19] As long as gold atoms participate in the small neck region of the break junction, conduction can be provided via Au-derived s and d states. If a single Ag atom forms the junction, electronic current can be transmitted via the Ag s channel. However, if Pd is present, the s channel is not easily accessible for ballistic transport, and accordingly one conductance quantum less is measured.

B. Electron density difference maps

Figure 4 gives electron density difference maps again for the most stable wires, i.e., the (8,4) systems Au_9, $AgAu_8$, and

$PdAu_8$. Both the Au_8 shell and the central metal chain experience a redistribution of the electron density due to the intershell interaction. For all three metals, a rehybridization occurs at the metal centers, which leads to a stronger localization of the electronic charge within and along the wire. This effect is most pronounced for the central atom chain, whose electron density becomes enclosed by the outer Au_8 shell.

Different redistribution patterns are obtained for the three metals, which reflect the symmetry ("nature") of the central conductance channel. The charge accumulation at both Au and Pd exhibits the fourfold symmetry of a d-type level, whereas for Ag, a twofold symmetric electron enrichment is obtained, which bears more similarity with a p state. In line with the results from the band structure analysis, states with d-type symmetry on the Au_8 shell gain electron density. Thus, the d bands of the Au_8 shell are completely occupied and do no longer touch the Fermi level close to the Z point Otherwise, the effect of the interaction on the outer shell exhibits no dependence on the central metal.

Additionally, light grey areas between the atoms of the central chain and the atoms of the shell depict the electron accumulation, which causes the bonding between the chain and the shell. The modulations of this grey area along c indicate some degree of directionality of the intershell bonding along the metal-metal directions. This effect is most pronouced for Au as central metal, whereas both Ag and Pd induce a more homogeneous electron accumulation around the central chain. The grey areas between the atoms of the outer shell suggest that the bonding interactions in this region are not modified, whereas the darker contour between the atoms of the central wire imply, that the bonding along the chain is weakened. Thus, the unfavorable tensile stress on the central part is reduced and even the gold-coated Pd wire is stable with respect to the free flat $Au(111)$ surface.

V. SUMMARY AND CONCLUSIONS

Density-functional band-structure calculations were carried out for two-shell metallic nanowires from Au and from AgAu and PdAu alloys. All structures are local minima with respect to the heat of formation, but stable with respect to the energy of the free, uncurved $Au(111)$ surface. The optimum structure for all three systems consists of an outer shell with eight Au atoms arranged in two layers in the repeat unit, and a central monatomic chain of $M=Au,Ag,Pd$. The radii and repeat unit lengths of all three systems are very similar ($r \approx 3.05$ Å, $c \approx 2.68$ Å). The calculated values of the formation energy and of the intershell binding energy indicate that the stability of the structure increases in the order $PdAu_8 < Au_9 < AgAu_8$. This trend coincides with the tensile stress acting on the central monatomic chain.

From an analysis of the electron density redistribution upon formation of the two-shell wire from the central chain and the outer shell it is concluded, that the binding between the two shells is not strongly directional, especially in the alloyed wires. Nevertheless, the interatomic interaction along the central chain is weakened and the tensile stress along this direction is reduced. All three systems exhibit metallic conductivity along the wire. For Au_9 and $AgAu_8$ eight s-level derived bands constitute the conductance channels for ballistic electron transport. For the Pd-centered wire only the conductance channels from the Au_8 shell are present, whereas the central one is depopulated. These findings rationalize the results from conductivity measurements on break junctions from AgAu and PdAu alloys: good electronic conductivity occurs even for very thin AgAu junctions, whereas ultrathin PdAu junctions exhibit a significantly lower conductivity. From the present calculations it is deduced, that a monatomic Ag contact would still provide a conductance channel along the junction, which is missing in the monatomic Pd contact. This result also supports the assumption of a monatomic contact in the break junction experiment.

[1] P. M. Laufer and D. A. Papaconstantopoulos, Phys. Rev. B **35**, 9019 (1987).

[2] Z. W. Lu, S.-H. Wei, and A. Zunger, Phys. Rev. B **44**, 10 470 (1991).

[3] P. Weinberger, L. Szunyogh, and B. I. Bennett, Phys. Rev. B **47**, 10 154 (1993).

[4] R. I. R. Blyth, A. B. Andrews, A. J. Arko, J. J. Joyce, P. C. Canfield, and B. I. Bennett, Phys. Rev. B **49**, 16 149 (1994).

[5] T.-U. Nahm, R. Jung, J.-Y. Kim, W.-G. Park, S.-J. Oh, J.-H. Park, J. W. Allen, S.-M. Chung, Y. S. Lee, and C. N. Wang, Phys. Rev. B **58**, 9817 (1998).

[6] B. E. Koel, A. Sellidj, and M. T. Paffett, Phys. Rev. B **46**, 7846 (1992).

[7] J. Kuntze, S. Speller, W. Heiland, P. Deurinck, C. Creemers, A. Atrei, and U. Bardi, Phys. Rev. B **60**, 9010 (1999).

[8] A. Roudgar and A. Groß, Phys. Rev. B **67**, 033409 (2003).

[9] B. R. Sahu, G. Maofa, and L. Kleinman, Phys. Rev. B **67**, 115420 (2003).

[10] J. H. Hodak, A. Henglein, M. Giersig, and G. V. Hartland, J. Phys. Chem. B **104**, 11 708 (2000).

[11] Y.-W. Cao, R. Jin, and C. A. Mirkin (unpublished).

[12] C. S. Ah, S. D. Hong, and D.-J. Jang, J. Phys. Chem. B **105**, 7871 (2001).

[13] I. Srnovà-Zloufovà, F. Lednicky, A. Gemperle, and J. Gemperlovà, Langmuir **16**, 9928 (2000).

[14] H. Shi, L. Zhang, and W. Cai, J. Appl. Phys. **87**, 1572 (2000).

[15] S. Link, Z. L. Wang, and M. A. El-Sayed, J. Phys. Chem. B **103**, 3529 (1999).

[16] E. Cottancin, J. Lerme, M. Gaudry, M. Pellarin, J.-L. Vialle, M. Broyer, B. Prevel, M. Treilleux, and P. Melinon, Phys. Rev. B

62, 5179 (2000).

[17] S. Gemming and M. Schreiber, Z. Metallkd. **94**, 3153 (2003).

[18] A. Enomoto, S. Kurokawa, and A. Sakai, Phys. Rev. B **65**, 125410 (2002).

[19] J. W. T. Hemskeerk, Y. Noat, D. H. J. Bakker, J. M. van Ruitenbeek, B. J. Thijsse, and P. Klaver, Phys. Rev. B **67**, 115416 (2003).

[20] P. Hohenberg and W. Kohn, Phys. Rev. **136**, B864 (1964).

[21] W. Kohn and L. J. Sham, Phys. Rev. **140**, A1133 (1965).

[22] D. M. Ceperley and B. J. Alder, Phys. Rev. Lett. **45**, 566 (1980).

[23] J. P. Perdew and A. Zunger, Phys. Rev. B **23**, 5048 (1981).

[24] The ABINIT code is a common project of the Universite Catholique de Louvain, Corning, Inc., and other contributors.

[25] C. Hartwigsen, S. Goedecker, and J. Hutter, Phys. Rev. B **58**, 3641 (1998).

[26] E. Tosatti, S. Prestipino, A. dal Corso, S. Köstlmeier, and F. di Tolla, Science **291**, 288 (2001).

[27] V. Rodriguez, T. Fuhrer, and D. Ugarte, Phys. Rev. Lett. **85**, 4124 (2000).

[28] V. Rodriguez, J. Bettini, A. R. Ocha, L. G. C. Rego, and D. Ugarte, Phys. Rev. B **65**, 153402 (2002).

[29] R. J. Needs and M. Mansfield, J. Phys.: Condens. Matter **1**, 7555 (1989).

[30] H. Bulou and C. Goyhenex, Phys. Rev. B **65**, 045407 (2002).

[31] U. Tartaglino and E. Tosatti, D. Passerone, and F. Ercolessi, Phys. Rev. B **65**, 241406 (2002).

[32] F. J. Ribeiro and M. L. Cohen, Phys. Rev. B **68**, 035423 (2003).